Chemical Engineering Journal 165 (2010) 545–553

Contents lists available at ScienceDirect

Chemical Engineering Journal

journal homepage: www.elsevier.com/locate/cej

Simulation and optimization of MSF desalination process for fixed freshwater demand: Impact of brine heater fouling

E.A.M. Hawaidi, I.M. Mujtaba*

School of Engineering Design & Technology, University of Bradford, Richmond Road, Bradford, West Yorkshire BD7 1DP, UK

ARTICLE INFO

Article history:
Received 17 May 2010
Received in revised form
28 September 2010
Accepted 29 September 2010

Keywords:
MSF desalination process
Brine heater fouling
Fixed water demand
Annual operating cost
Simulation
Optimization

ABSTRACT

The most costly design and operation problems in seawater desalination are due to scale formation and corrosion of plant equipment. Fouling factor (a measure of scale formation) is one of the many important parameters that affect the operation of MSF processes. In this work, a steady state model of MSF is developed based on the basic laws of mass balance, energy balance, and heat transfer equations with supporting correlations for physical properties calculations. The model includes parameters such as the brine flow rate, freshwater flow rate, the temperature profiles for all stages, top brine temperature and steam flow rate. gPROMS model builder 2.3.4 software is used for model development, simulation and optimization. The model is validated against the simulation results reported in the literature. The model is then used to study the role of a changing brine heater fouling factor with varying seawater temperatures and its effect on the plant performance for fixed water demand, for a given steam and top brine temperature.

For fixed water demand, this paper also studies the effect of brine heater fouling factor with seasonal variation of seawater temperatures on the operating cost. Based on actual plant data, a simple linear dynamic fouling factor profile is developed which allows calculation of fouling factor at different time (season of the year). January is considered to be the starting time (when the fouling factor is minimum) of the process after yearly overhauling. The total monthly operation cost of the MSF process is selected to minimize, while optimizing the operating parameters such as make up, brine recycle flow rate and steam temperature. This leads to a seasonal optimal operation policy for the whole year.

1. Introduction

About 40% of the world's population suffer from a shortage of fresh water and this trend is expected to increase in the future. Among various desalination processes, the multistage flash (MSF) desalination process is a thermal process and is a major source of fresh water around the world [1].

Water with soluble salts at high temperature allows deposits to form. This is commonly referred to as 'scale' or 'foul' which can be defined as crystalline growth of an adherent layer (barrier) of sparingly soluble salts that can readily precipitate on a heat transfer surface in evaporative operation. The rate of scale formation is a complicated function of many variables such as temperature, pH and concentration of salts. Scale formation is mainly caused by crystallization of calcium carbonate e.g. $CaCO_3$ and magnesium hydroxide $Mg(OH)_2$. Non-alkaline scales e.g. $CaSO_4$ are perhaps the most common scales found in multi stage flash (MSF) [2]. However, fouling can reduce the heat transfer rate reducing heat transfer efficiency by plugging the exchangers. In addition, fouling can increase specific energy consumption and operating costs and can also cause frequent shutdowns of the evaporator for cleaning. Scaling and corrosion can lead to more costly designs and operating problems in seawater desalination. The fouling tendency requires about 20–25% excess design allowance [3] and the design of the heat transfer area constitutes about 30% of the total cost.

Even though high top brine temperature (TBT) operation increases the efficiency of the plant, it increases the potential for scale formation and accelerates the corrosion rate of metal surfaces [4]. Practical experience shows that the fouling formation rate can be significantly increased inside the condensers and brine heater tubes and leading to shutdown of the plant for cleaning when the plant operates at high TBT = 115 °C [5]. The accurate calculation of the overall heat transfer coefficient (which is also a function fouling factor) is of substantial importance in MSF processes. Scaling leads to dynamic adjustment of operating conditions if certain freshwater demand is to be met. Rather than playing with an operating plant to determine the new set points it is always economical to determine the optimal set points based on accurate process model and optimization techniques before the operating set-points are applied in the actual plant [6].

* Corresponding author.
E-mail address: I.M.Mujtaba@bradford.ac.uk (I.M. Mujtaba).

1385-8947/$ – see front matter © 2010 Elsevier B.V. All rights reserved.
doi:10.1016/j.cej.2010.09.071

Nomenclature

A_H	heat transfer area of brine heater (m^2)
A_J	heat transfer area of stage j (m^2)
B_0	flashing brine mass flow rate leaving brine heater (kg/h)
BBT	bottom brine temperature (°C)
B_D	blow-down mass flow rate (kg/h)
BHF	brine heater fouling factor (m^2 h K/kcal)
B_J	flashing brine mass flow rate leaving stage j (kg/h)
B_{NS}	flashing brine mass flow rate leaving last stage j (kg/h)
CP_{Bj}	heat capacity of flashing brine leaving stage j (kcal/kg °C)
CP_{Dj}	heat capacity of distillate leaving stage j (kcal/kg °C)
CP_j	heat capacity of cooling brine leaving stage j (kcal/kg °C)
CP_{RH}	heat capacity of brine leaving brine heater (kcal/kg °C)
C_W	rejected seawater mass flow rate (kg/h)
D_J	distillate flow rate leaving stage j (kg/h)
D_N	total distillate flow rate (kg/h)
F	make-up seawater mass flow rate (kg/h)
f_{bh}	brine heater fouling factor (m^2 h/kw)
f_j	fouling factor at stage j (m^2 h/kw)
GOR	gained out ratio or performance ratio
h_{Bj}	specific enthalpy of flashing brine at stage j (kcal/kg)
h_F	specific enthalpy of make-up water (kcal/kg)
H_j	height of brine pool at stage j (m)
h_M	specific enthalpy of brine at T_{FM} (kcal/kg)
h_R	specific enthalpy of flashing brine recycle (kcal/kg)
h_{vj}	specific enthalpy of flashing vapor at stage j (kcal/kg)
ID	internal diameter of tubes (m)
L_H	length of brine heater tubes (m)
L_J	length of tubes at stage j (m)
OD	external diameter of tubes (m)
R	recycle stream mass flow rate (kg/h)
T_{BJ}	temperature of flashing brine leaving stage j (°C)
T_{BNS}	temperature of blow-down (°C)
T_{BO}	temperature of flashing brine leaving brine heater (°C)
TBT	top brine temperature (°C)
T_{DJ}	temperature of distillate leaving stage j (°C)
TE_J	boiling point elevation at stage j (°C)
T_{FJ}	temperature of cooling brine leaving stage j (°C)
T_{FM}	temperature of cooling brine to the heat recovery section (°C)
T_{FNR}	temperature of make-up (°C)
$T_{seawater}$	seawater temperature (°C)
T_{steam}	steam temperature (°C)
T_{VJ}	temperature of flashed vapour at stage j (°C)
U_H	overall heat transfer coefficient at brine heater (kcal/m^2 h K)
U_J	overall heat transfer coefficient at brine heater (kcal/m^2 h K)
V_J	linear velocity of brine (m/s)
W_J	width of stage (m)
W_R	cooling brine mass flow rate to the heat recovery section (kg/h)
W_S	seawater mass flow rate (kg/h)
W_{steam}	steam mass flow rate (kg/h)
X	salt concentration (wt.%)
X_{BJ}	salt concentration in flashing brine leaving stage j (wt.%)
X_{BNS}	salt concentration in flashing brine leaving last stage (wt.%)
X_F	salt concentration in make-up water (wt.%)
X_R	salt concentration in cooling brine (wt.%)
X_S	salt concentration in seawater (wt.%)
$\triangle_j$	temperature loss due to demister (°C)
ρ_j	brine density (kg/m^3)
λ_s	latent heat of steam to the brine heater (kcal/kg)
δ	non-equilibrium of tubes (°C)

Index

H	brine heater
J	stage index
*	reference value

In this work, the effect of changing of brine heater fouling with varying seawater temperature on plant performance, TBT, brine flow rate, amount of recycle and steam required for fixed water demand under fixed steam temperature operation by MSF desalination process are studied using mathematical process model. In the past several modelling, simulation and optimization studies of MSF process have been carried out using fixed fouling factor for the brine heater [1,6,7]. However, in this work, a time dependent fouling factor (to represent dynamic scaling effect) is also developed and a series of optimal operation snap shots are taken at discreet time intervals. In addition to simulation, an optimization problem is formulated by incorporating the steady state process model and the operating cost is minimized while the operation parameters (such as make up, brine recycle flow rate and steam temperature) are optimized for a given configuration of the MSF process and a given fresh water demand.

2. Understanding scaling and fouling factor

Calcium carbonate is perhaps the most common scale found in water systems. However, as the temperature increases the solubility of calcium carbonate decreases. Calcium carbonate scale is formed by the combination of calcium ion with either carbonate or bicarbonate ions as follows:

$$CO_2 + OH^- \rightleftarrows HCO_3^- \quad \text{athighpHvalues}(pH > 8.8) \tag{1}$$

$$HCO_3^- + OH^- \rightleftarrows CO_3^{2-} + H_2O \tag{2}$$

$$Ca^{2+} + CO_3^{2-} \rightarrow CaCO_3\downarrow \tag{3}$$

$$Ca^{2+} + 2(HCO_3^-) \rightarrow CaCO_3\downarrow + H_2O + CO_2 \tag{4}$$

The CO_2 release rates increase with increasing TBT and $CaCO_3$ deposition and thus the fouling factor is increased. $CaCO_3$ deposition rates 76.9–123.0 g m/t of distillate at 90–110 °C corresponding to 0.64–1.0 m^2 K/kw (0.000745–0.00118 h m^2 K/kcal) respectively [8]. Note, these fouling factor values are very high compared to that used (fouling factor = 0.000186 h m^2 K/kcal, =0.159 m^2 K/kw) in Rosso et al. [9] who used 'polyphosphonates' as anti scaling at seawater temperature = 35 °C and TBT = 90 °C.

3. MSF process configuration

A typical MSF plant is shown in Fig. 1. The process consists of essentially a steam source, water/steam circuit (brine heater), pumping units and flashing stages sections. The seawater is pumped through the condenser tubes from the end of the rejection

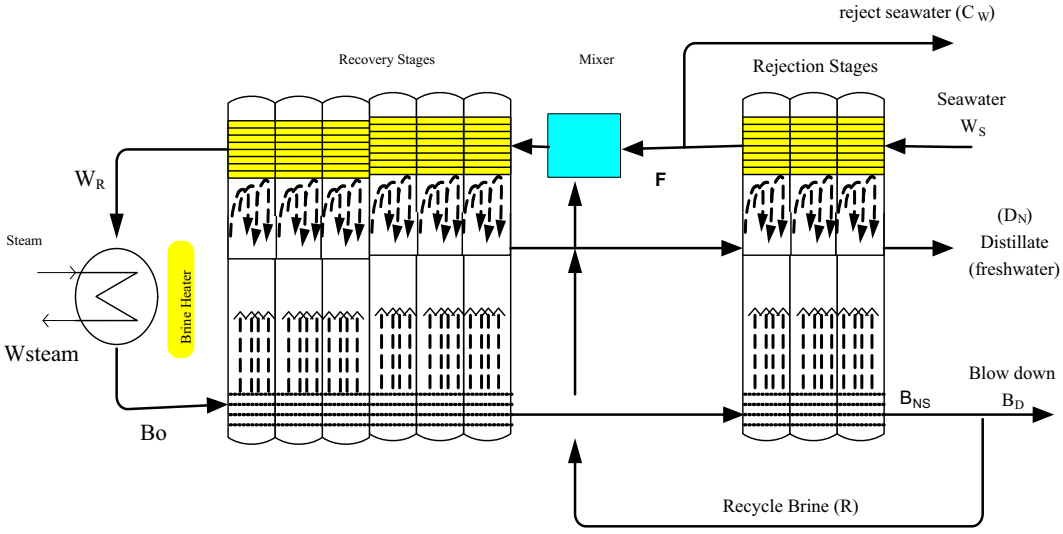

Fig. 1. A typical MSF process.

section to the left of the section. Before the recovery section, seawater is partially discharged into the sea to balance the heat. The other part is treated with a mixture of anti-scaling such as 'polyphosphonates', sulphuric acid and chlorination compounds and is mixed with recycled brine and fed into the last stage of the recovery section and is preheated in the condenser units by exchanging heat with the distillate vapour. The preheated seawater is further heated in the brine heater and flows into the first flash chamber with the highest possible temperature (TBT) and low pressure. However, the brine partly flashes into vapour upon entering the next stage and condenses on the condenser tubes. The condensed vapour accumulates and flows in the distillate tray across the stages. The brine is divided into a blow down stream and a recycle stream, which is combined with the make-up water and enters the heat recovery section.

Note, due to high temperature in the recovery stages and brine heater, seawater is treated with anti-scaling and assisted by sponge ball cleaning to reduce scale formation. Acid cleaning is required after more than a year in operation [10].

Each stage of an MSF evaporator (Fig. 2) consists of:

- The tube bundles of the condenser to condense the vapour in the stage.
- The demister to reject brine droplets.
- The distillate tray to collect the distillate water.
- Inlet/outlet brine orifices and a weir box to control flashing brine level.
- An extraction pipe leading to ejectors to remove non- condensable gases.
- A large brine pool.

4. MSF process model

Numerous studies on modelling and simulation of MSF desalination process are available in the literature [9,11–16]. Many models have been developed to analyse the MSF water desalination process. All of these models are developed from the basic of mass, energy balance and heat transfer equations. In addition, these models are supported by equations for calculating the thermal and physical properties of brine and distillate waters as functions of temperature and salt concentration.

The assumptions used to develop the mathematical model include the following:

- Steady state operation.
- Heat losses to the surroundings are negligible.
- The heat capacities, specific enthalpies and physical properties for feed seawater, brine and distillate product are functions of temperature and composition.
- The fouling resistance is constant for recovery and rejection section.
- Thermodynamic losses include the boiling point elevation (TE), the non-equilibrium allowance (δ) and demister losses (Δ).
- The distillate product is salt free.
- Heat of mixing is negligible.
- No sub-cooling of condensate leaving the brine heater.

The model equations are constituted of a set of mass and energy balances which are given in the following (all symbols are defined in the list of symbols). All physical properties correlation are taken from Rosso et al. [9] except the temperature elevation (TE) due to salinity which is taken form EL-Dessouky and Ettouney [1]. Rosso et al. [9] used TE correlation from Stoughton and Lietzke [17]

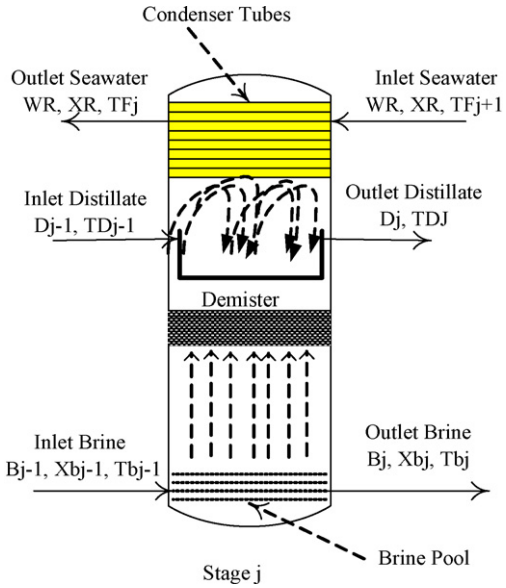

Fig. 2. Typical flash stage.

and is accurate within salinity range of 3.45–20% and temperature 30–250 °C. The TE correlation used by EL-Dessouky and Ettouney [1] is accurate within the salinity range 1–16% and temperature 10–180 °C. Since the salinity and temperature range of our work fall within these limits we have used this correlation in this work.

4.1. Stage model

Mass balance in the flash chamber : $B_{j-1} = B_j + D_j$ (5)

The stage salt balance is given by : $X_{bj}B_j = X_{bj-1}B_{j-1}$ (6)

Mass balance for distillate tray : $$\sum_{k=1}^{j} D_k = \sum_{k=1}^{j-1} D_k + D_j \quad (7)$$

Enthalpy balance on flash brine : $$\frac{B_j}{B_{j-1}} = \frac{(h_{Bj-1} - h_{vj})}{(h_{Bj} - h_{vj})}$$

$$h_{vj} = f(T_{Vj}) \quad h_{Bj} = f(T_{Bj}, X_{Bj}) \quad (8)$$

Overall energy balance on stage : $W_R cp_j(T_{Fj} - T_{Fj+1})$

$$= \sum_{k=1}^{j-1} D_k cp_{Dj-1}(T_{Dj-1} - T^*) - \sum_{k=1}^{j} D_k cp_{Dj}(T_{Dj} - T^*)$$

$$+ B_{j-1} cp_{Bj-1}(T_{Bj-1} - T^*) - B_j cp_{Bj}(T_{Bj} - T^*) \quad (9)$$

Heat transfer equation : $W_R cp_j(T_{Fj} - T_{Fj+1}) = U_j A_j LMTD_j$ (10)

The logarithmic mean temperature difference in the recovery stage is : $$LMTD_j = \frac{(T_{Fj} - T_{Fj+1})}{\ln((T_{Dj} - T_{FJ+1})/(T_{DJ} - T_{Fj}))} \quad (11)$$

where U_J is calculated in terms of W_R, T_{Fj}, T_{Fj+1}, T_{Dj}, ID, OD and f_j

$cp_j = f(T_{FJ+1}, T_{Fj}, X_R)$, $CP_{Bj} = f(T_{Bj}, X_{Bj})$, $CP_{Dj} = f(T_{Dj})$

Distillate and flashing brine temperature correlation : $T_{Bj} = T_{Dj} + TE_j + \Delta_j + \delta_j$ (12)

where,

$\Delta_j = f(T_{Dj})$, $TE_j = f(T_{Bj}, X_{Bj})$, $\delta_j = f(T_{BJ}, H_J, W_j)$

Distillate flashed steam temperature correlation : $T_{Vj} = T_{Dj} + \Delta_j$ (13)

4.2. Brine heater model

$B_0 = W_R$, $X_{B0} = X_R$ (14)

$B_0 CP_{RH}(T_{B0} - T_{FI}) = W_{steam}\lambda_s$ (15)

$\lambda_s = f(T_{steam})$ (16)

Heat transfer equation : $W_R(T_{B0} - T_{F1}) = U_H A_H LMTD$ (17)

The logarithmic mean temperature difference in brine heater is : $$LMTD_j = \frac{(T_{B0} - T_{F1})}{\ln((T_{steam} - T_{F1})/(T_{steam} - T_{B0}))} \quad (18)$$

where U_H is calculated in terms of W_R, T_{Fj}, T_{B0}, T_{steam}, ID, OD and f_{bh}

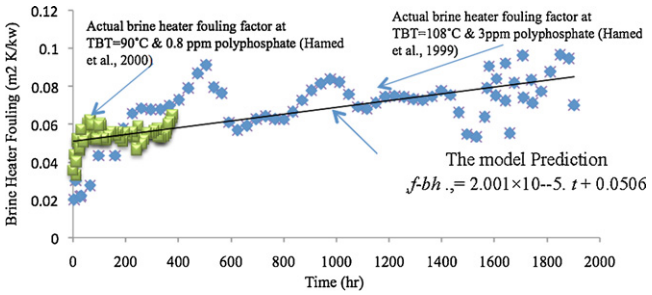

Fig. 3. Brine heater fouling f_{bh} profile.

4.3. Splitters model

$B_D = B_{NS} - R$ $C_W = W_s - F$ (19)

4.4. Makeup mixers models

$W_R = R + F$ $RX_{BNS} + FX_F = W_R X_R$ (20)

$W_R h_M = Rh_R + Fh_F$ (21)

where,

$h_M = f(T_{FM}, X_R)$, $h_F = f(T_{FNR}, X_F)$, $h_R = f(T_{BNS}, X_{BNS})$

4.5. Plant performance measure

$$\text{GOR} = \frac{D_N}{W_{steam}} \quad (22)$$

5. Estimation of dynamic brine heater fouling profile

Fig. 3 shows the variation of actual fouling factor (m^2 K/kw) with time (h) of the brine heater section [18,19]. Using regression analysis, the following linear relationship is obtained (also shown in Fig. 3). Note, high dosing is required for high TBT to keep the fouling factor at the same level of low dosing and low TBT case.

$$f_{bh} = 2.001 \times 10^{-5} t + 0.0506 \quad (23)$$

The constant 0.0506 in Eq. (23) represents the initial fouling of the brine heater section (f_{bh}, m^2 K/kw) at $t = 0$ (say January, at the beginning of the operation after the plant overhauling). In this work, the trend of brine heater fouling f_{bh} profile is assumed to be valid for the whole year (i.e. 8000 h).

Note, the actual fouling data in Fig. 3 could have been fitted with a polynomial which could be used within the time horizon 0–2000 h. Beyond 2000 h a polynomial based expression predicts abnormally high value of fouling.

6. Model validation

The case study reported by Rosso et al. [9] (which was based on industrial data) is used here for model validation. The configuration investigated in this work includes 13 stages in heat recovery section and 3 stages in the heat rejection section.

The specifications and constant parameters used by Rosso et al. [9] and this work are shown in Table 1. The summary of the simulation results by Rosso et al. [9] (shown in plain) and this work (shown in italic) are presented in Table 2. Both models calculate the brine flow rate, fresh water and the temperature profiles for all stages, top brine temperature and steam flow rate. A comparison of the results in Table 2 shows that there is an excellent agreement between them. Slight differences in the results are due to the use of different correlation for temperature elevation due to salinity.

Table 1
Constant parameters and input data.

	A_j/A_H	ID_j/ID_H	OD_j/OD_H	f_j/f_{bh}	w_j/L_H	H_j
Brine heater	3530	0.022	0.0244	0.159	12.2	–
Recovery stage	3995	0.022	0.0244	0.120	12.2	0.457
Rejection stage	3530	0.024	0.0244	0.020	10.7	0.457

W_S (kg/h)	T_{steam} (°C)	$T_{seawater}$ (°C)	X_S (wt.%)	R (kg/h)	C_W (kg/h)
1.131×10^7	97	35	5.7	6.35×10^6	5.62×10^6

Table 2
Summary of the simulation results.

F (kg/h)	B_D (kg/h)	W_R (kg/h)	W_{steam} (kg/h)	X_R (wt.%)
5.68×10^6	4.74×10^6	1.203×10^7	1.348×10^5	6.29
5.68×10^6	*4.74×10^6*	*1.203×10^7*	*1.360×10^5*	*6.29*

Stage	B_j (kg/h)	D_j (kg/h)	XB_j (wt.%)	TF_j (°C)	TD_j (°C)	TB_j (°C)	U_j (kcal/h m² k)
Stage profiles (brine heater stage $j=0$; $TBT=T_{B0}$)							
0	1.203E+07		6.2922			89.74	2040.9
	1.203E+07		*6.2946*			*89.71*	*2048.9*
1	1.197E+07	5.940E+04	6.3234	83.33	85.75	86.89	2250.0
	1.197E+07	*5.8915E+4*	*6.3256*	*83.25*	*85.68*	*86.86*	*2257.0*
2	1.191E+07	1.187E+05	6.3549	80.41	82.87	84.01	2246.4
	1.191E+07	*1.184E+05*	*6.3572*	*80.29*	*82.77*	*83.97*	*2253.5*
3	1.185E+07	1.784E+05	6.3869	77.44	79.95	81.08	2243.0
	1.185E+07	*1.784E+05*	*6.3894*	*77.29*	*79.81*	*81.03*	*2250.3*
4	1.179E+07	2.385E+05	6.4195	74.43	76.97	78.11	2239.9
	1.179E+07	*2.388E+05*	*6.4221*	*74.26*	*76.80*	*78.05*	*2247.3*
5	1.173E+07	2.989E+05	6.4525	71.37	73.94	75.09	2236.9
	1.173E+07	*2.994E+05*	*6.4553*	*71.18*	*73.75*	*75.03*	*2244.5*
6	1.167E+07	3.595E+05	6.486	68.28	70.88	72.04	2234.2
	1.167E+07	*3.602E+05*	*6.4889*	*68.08*	*70.67*	*71.98*	*2242.0*
7	1.161E+07	4.201E+05	6.5198	65.16	67.78	68.95	2231.7
	1.161E+07	*4.211E+05*	*6.5230*	*64.95*	*67.56*	*68.91*	*2239.6*
8	1.155E+07	4.806E+05	6.554	62.01	64.65	65.84	2229.2
	1.155E+07	*4.819E+05*	*6.5573*	*61.80*	*64.42*	*65.81*	*2237.4*
9	1.149E+07	5.410E+05	6.5885	58.84	61.49	62.7	2226.2
	1.149E+07	*5.425E+05*	*6.5919*	*58.64*	*61.26*	*62.71*	*2235.1*
10	1.143E+07	6.010E+05	6.6231	55.65	58.32	59.55	2224.0
	1.143E+07	*6.029E+05*	*6.6267*	*55.46*	*58.10*	*59.59*	*2232.6*
11	1.137E+07	6.606E+05	6.6578	52.46	55.13	56.39	2221.0
	1.137E+07	*6.628E+05*	*6.6617*	*52.29*	*54.92*	*56.48*	*2229.9*
12	1.131E+07	7.197E+05	6.6925	49.27	51.93	53.24	2217.6
	1.131E+07	*7.222E+05*	*6.6966*	*49.11*	*51.74*	*53.37*	*2226.7*
13	1.125E+07	7.780E+05	6.7272	46.09	48.74	50.09	2213.6
	1.125E+07	*7.786E+05*	*6.7302*	*45.95*	*48.69*	*50.39*	*2222.5*
14	1.120E+07	8.296E+05	6.7582	44.06	45.87	47.28	2917.3
	1.120E+07	*8.306E+05*	*6.7615*	*44.09*	*45.84*	*47.62*	*2988.4*
15	1.115E+07	8.816E+05	6.7897	41.1	42.95	44.42	2905.9
	1.115E+07	*8.836E+05*	*6.7936*	*41.13*	*42.92*	*44.79*	*2978.6*
16	1.110E+07	9.341E+05	6.8219	38.07	39.98	41.51	2892.3
	1.109E+07	*9.373E+05*	*6.8265*	*38.09*	*39.94*	*41.90*	*2966.4*

7. Effect of brine heater fouling on the performance

7.1. Fixed seawater temperature, steam temperature and steam consumption rate

With the model (validated above), a series of simulations have been carried out to study the sensitivity of Brine Heater Fouling (f_{bh}) on the performance of MSF processes (defined in Eq. (22)) for fixed steam temperature (T_{steam} = 97°C), fixed steam consumption (W_{steam} = 135,000 kg/h) and fixed seawater temperature ($T_{seawater}$ = 35 °C). The f_{bh} is assumed to vary between 0.0 and 3.5×10^{-4} h m² K/kcal (0.0–0.30114 m² K/kw). The other input data, which are fixed for all cases, are shown in Table 1.

Fig. 4 illustrates the effect of f_{bh} on TBT and distilled water production rate (D_N). It is clear from the figure that TBT is strongly dependent of the f_{bh} i.e. as the fouling factor increases the TBT decreases and consequently the distilled water production rate decreases.

Figs. 5–7 represent the effect of the f_{bh} on temperature profiles of brine and fresh water through all the stages (stage-by-stage). These figures demonstrate that the temperatures (T_{Fj}, T_{Bj}, and T_{Dj}) are completely dependent on f_{bh}. As f_{bh} increases, the temperatures decrease. As TBT (=TB0) is different for different f_{bh}, each T_{Bj}

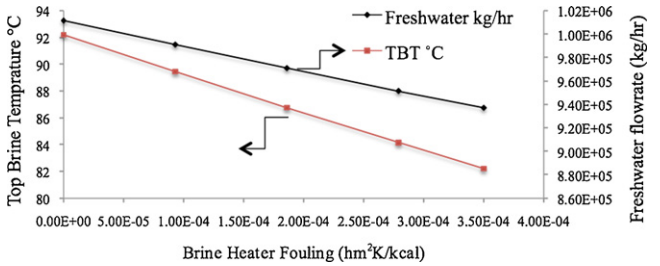

Fig. 4. Effect of brine heater fouling factor on freshwater flow rate and TBT at fixed steam temperature and fixed steam consumption.

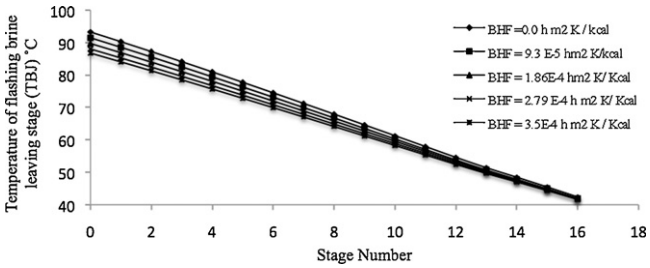

Fig. 5. Temperature variation of brine through stages.

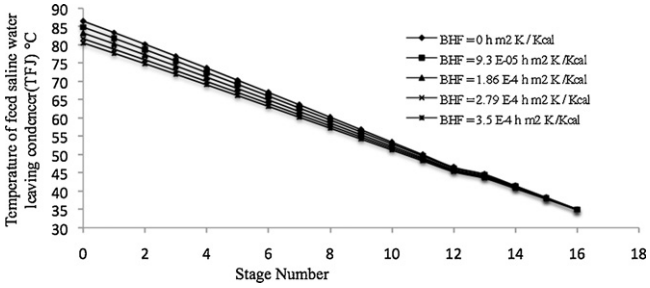

Fig. 6. Temperature variation of feed saline water through condenser.

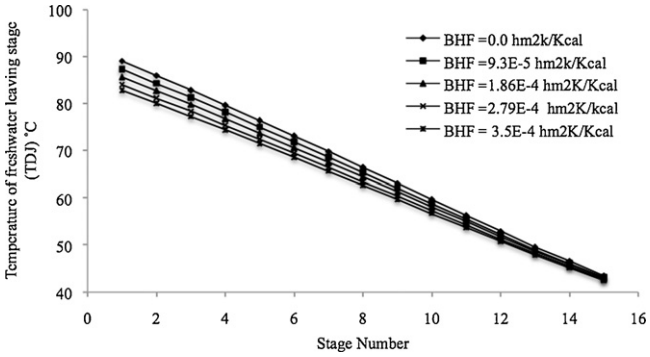

Fig. 7. Temperature variation of freshwater through stages.

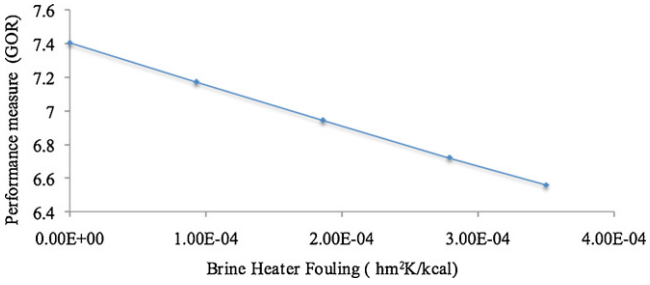

Fig. 8. Effect of brine heater fouling on plant performance (GOR).

profiles are different with wider gap in temperature at the beginning but converging to a single value at the last stage due to the fixed seawater temperature for all cases. This is true for T_{Fj} and T_{Dj} profiles.

Fig. 8 illustrates the effect of increasing f_{bh} on plant performance (GOR) with fixed steam temperature and steam consumption rate. Increase in f_{bh} reduces in the overall heat transfer coefficient and the TBT leading to a reduction in the distilled water production (as shown in Fig. 4) accompanied by a reduction in the performance as shown in Fig. 8. The production rate decreases by about 5.5%, and therefore the performance ratio decreases by 5.5% as the

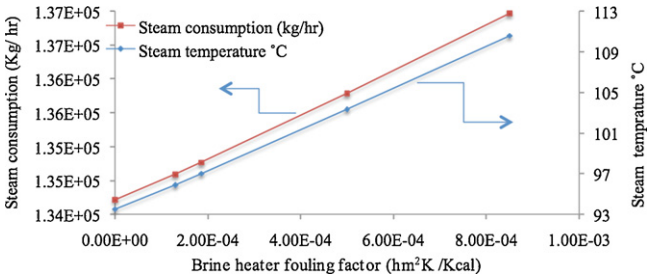

Fig. 9. Effect of brine heater fouling factor on steam consumption and steam temprature.

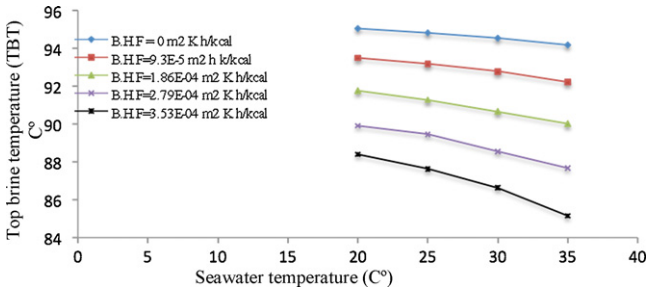

Fig. 10. Effect of the brine heater fouling on top brine temperature (TBT).

f_{bh} increases from 1.84×10^{-4} to 3.5×10^{-4} h m^2 K/kcal (about 90% increase). Attention should be paid to the brine heater fouling factor since this plays a critical role in the calculation of heat transfer.

7.2. Fixed seawater temperature, top brine temperature (TBT) and fresh water demand

For the purpose of better understanding of the effect of $CaCO_3$ deposit (without use of anti-scalant) further simulation is carried out to study of sensitivity of f_{bh} on the performance of the MSF process with fixed seawater temperature ($T_{seawater} = 35\,^{\circ}C$), fresh water demand ($D_N = 9.341 \times 10^5$ kg/h) and TBT = 90 °C.

Fig. 9 shows the effect of f_{bh} on the steam temperature (T_{steam}) and steam flow rate (W_{steam}), while the f_{bh} increases form 1.84×10^{-4} [9] to 7.53×10^{-4} h m^2 K/kcal [8]. About 1.5% increase in steam consumption and corresponding increase in steam temperature by 12% are noted. According to Eq. (22) the performance ratio decreases also by 1.75%.

7.3. Variable seawater temperature, fixed freshwater demand and fixed steam temperature

The brine heater fouling is assumed to vary between 0.0 and 3.53×10^{-4} h m^2 K/kcal (0–0.3 m^2 K/kw) and the seawater temperature from 20 and 35 °C [20]. The sensitivity of brine heater fouling (f_{bh}) on the performance of the MSF processes with fixed steam temperature ($T_{steam} = 97\,^{\circ}C$) and fixed fresh water ($D_N = 9.45 \times 10^5$ kg/h) are shown in Figs. 10–14.

Fig. 10 represents the effect of f_{bh} on TBT with changing seawater temperatures from winter to summer season. For a given f_{bh}, TBT decreases as seawater temperature increases. However, interestingly (and not reported elsewhere to the best of the author's knowledge) it can be noted that the plant can operate a lower TBT at higher brine heater fouling producing the same amount of freshwater.

Fig. 11 illustrates the effect of f_{bh} on steam consumption. It is clear from the figure that the steam consumption increases as the fouling factor and the seawater temperature increase, due to drop in TBT (shown in Fig. 10). This is required to maintain the

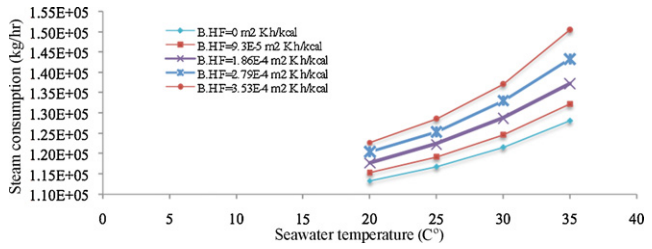

Fig. 11. Effect of brine heater fouling on steam flow rate.

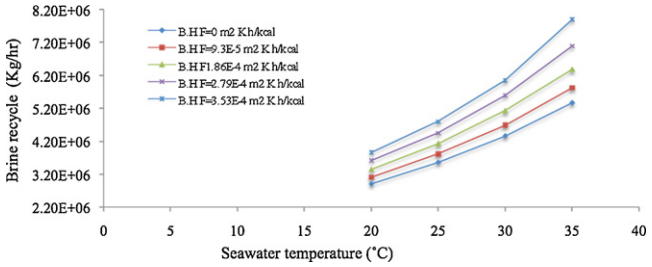

Fig. 12. Effect of brine heater fouling on brine recycle flow rate.

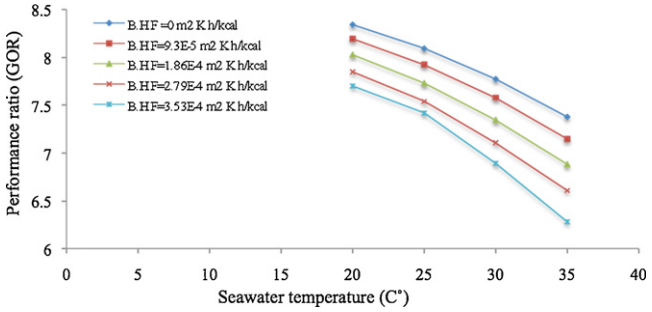

Fig. 13. Effect of brine heater fouling on performance.

freshwater production at the desired level. Also note, higher TBT requires a lower amount of steam at any seawater temperature (Figs. 10 and 11). It is interesting to reflect that when seawater temperature in fixed, steam temperature needs to increase together with steam consumption (Fig. 9) with increasing f_{bh}. However, when seawater temperature increases, steam consumption needs to be increased with increasing f_{bh} but steam temperature can be kept constant (Fig. 11).

Fig. 12 demonstrates that the amount of brine recycling (kg/h) increases with increased brine heater fouling and seawater temperature.

Comparison of Figs. 10–12 reveal that at any seawater temperature, increase of f_{bh} (i) decreases TBT, (ii) increases steam consumption and (iii) increases brine recycling to maintain the freshwater production at the desired level.

Fig. 13 shows the effect of increasing brine heater fouling factor on the performance ratio. Here, the reduction in the TBT results in increases in the steam flow rate as shown in Figs. 10 and 11, accompanied by a reduction in the performance. For example at seawater temperature 20 °C the amount of steam increases by 4.2%, and the performance ratio decreases by 4% as the brine heater fouling changes from 1.86×10^{-4} m^2 h K/kcal to maximum value. Furthermore, the brine recycle rate will increase at about 15% and TBT decreases by 3.3 °C.

Table 3
Pre- treatments for make-up.

Chemical	Unit cost ($/kg)	Dosing rate (ppm)
Sulphuric acid, H_2SO_4	0.504	24.2
Caustic soda—NaOH	0.701	14
Anti-scaling of polyphosphonates	1.9	(0.8 or 3)
Chlorine	0.482	4

8. Effect of brine heater fouling on optimization of operation parameters

8.1. Optimization problem formulation

The optimization problem is described below.

Given: Fixed number of stages, heat exchangers areas, design specification of each stages, seawater flow and fixed freshwater demand.

Optimize: Steam temperature (T_{steam}), Recycled brine flow rate (R), Make-up seawater (F).

Minimize: The total annualized operating cost (TOC).

Subject to: Any constraints.

The Optimization Problem (OP) can be described mathematically by:

$$OP \quad \underset{T_{steam},R,F}{Min} \quad TOC$$

$$\text{s.t.} \quad f(x,u,v) = 0 \quad (\text{model equations})$$
$$D_N = D_N^*$$
$$\text{TBT} = \text{TBT}^*$$
$$(92\,^\circ C) \quad T_{steam}^L \le T_{steam} \le T_{steam}^U (115\,^\circ C)$$
$$(2 \times 10^6) \quad R_L \le R \le R_U (5.5 \times 10^6)$$
$$(1.5 \times 10^6) F_L \le F \le F_U \quad (6.8 \times 10^6)$$

where D_N is the total amount of fresh water produced and D_N^* is the fixed water demand (9.45×10^5 kg/h). TBT* is the fixed TBT (90 or 108 °C). Subscripts L/superscripts U refer to lower and upper bounds of the parameters. The model equations presented in Section 4 can be described in a compact form by $f(x,u,v) = 0$ where x represents non-linear sets of all algebraic variables, u is the optimization variable, such as steam temperature, recycle flow rate, etc., v is a set of constant parameters such as number of stages, heat exchangers areas, etc.Total Annualized Operating Cost can be described [21]:

$$\text{TOC (Total Annualized Operating Cost, \$/year)} = C1 + C2 + C3 + C4 + C5 \tag{24}$$

where

$$C1 \ (\text{Steam cost}) = 8000 \times W_{steam} \times \left[(T_{steam} - 40)/85\right] \times 0.00415 \tag{25}$$

$$C2 \ (\text{Chemical cost}) = 8000 \times \left[\sum (\text{Unit cost} \left(\frac{\$}{g}\right) \times \text{Dosing rate (ppm)}) \times \frac{F}{Db}\right] \tag{26}$$

where Db = density of brine (kg/m^3).

Chemical cost ($/kg) and dosing rate (ppm) [22] is given in Table 3

$$C3 \ (\text{Power cost}) = 8000 \times \left[\frac{D_N}{1000}\right] \times 0.109 \tag{27}$$

$$C4 \ (\text{Maintenance and spares cost}) = 8000 \times \left[\frac{D_N}{1000}\right] \times 0.082 \tag{28}$$

Table 4
Summary of optimization results (Case 1).

Months	$T_{seawater}$ (°C)	f_{bh} (m² K/kW)	$F \times 10^6$ (kg/h)	$R \times 10^6$ (kg/h)	T_{stam} (°C)	Anti-scale (kg/month)	TOC × 10^5 ($/month)	Steam (kg/h)	GOR
January	15	0.065	3.91	4.74	93.6	2252.2	4.48	116,955	8.08
February	17	0.078	4.09	4.78	94.0	2360.7	4.54	118,095	8.00
March	20	0.093	4.40	4.85	94.4	2539.9	4.65	120,122	7.86
April	25	0.108	5.02	4.98	95.2	2892.0	4.85	124,260	7.60
May	28	0.121	5.48	5.05	95.6	3159.0	5.01	127,307	7.42
June	30	0.135	5.80	5.13	96.1	3341.0	5.12	129,470	7.28
July	32	0.150	6.15	5.21	96.7	3542.0	5.25	132,241	7.14
August	35	0.164	6.75	5.35	97.4	3891.4	5.47	136,718	6.91
September	33	0.1780	6.34	5.26	97.5	3652.0	5.34	133,739	7.06
October	30	0.1920	5.79	5.13	97.4	3340.0	5.18	129,986	7.27
November	25	0.2060	5.02	4.98	97.2	2892.0	4.94	124,555	7.58
Total						33,862.2	54.83		

Table 5
Summary of optimization results (Case 2).

Months	$T_{seawater}$ (°C)	f_{bh} (m² K/kw)	$F \times 10^6$ (kg/h)	$R \times 10^6$ (kg/h)	T_{stam} (°C)	Anti-scale (kg/month)	TOC × 10^5 ($/month)	Steam (kg/h)	GOR
January	15	0.065	2.45	4.40	110.3	5309.1	4.52	98,823	9.56
February	17	0.078	2.47	4.42	110.7	5557.5	4.57	99,535	9.49
March	20	0.093	2.75	4.45	111.0	5952.9	4.64	100,677	9.38
April	25	0.108	3.09	4.52	111.4	6685.9	4.78	102,839	9.18
May	28	0.121	3.32	4.57	111.8	7177.2	4.87	104,345	9.05
June	30	0.135	3.48	4.60	112.1	7529.0	4.94	105,457	8.96
July	32	0.150	3.65	4.64	112.5	7902.8	5.01	106,657	8.86
August	35	0.164	3.94	4.71	112.9	8520.5	5.13	108,625	8.69
September	33	0.1780	3.75	4.67	113.1	8098.6	5.06	107,344	8.80
October	30	0.1920	3.48	4.60	113.2	7529.6	4.97	105,584	8.95
November	25	0.2060	3.04	4.52	113.1	6687.4	4.84	103,050	9.17
Total						76,950.5	53.33		

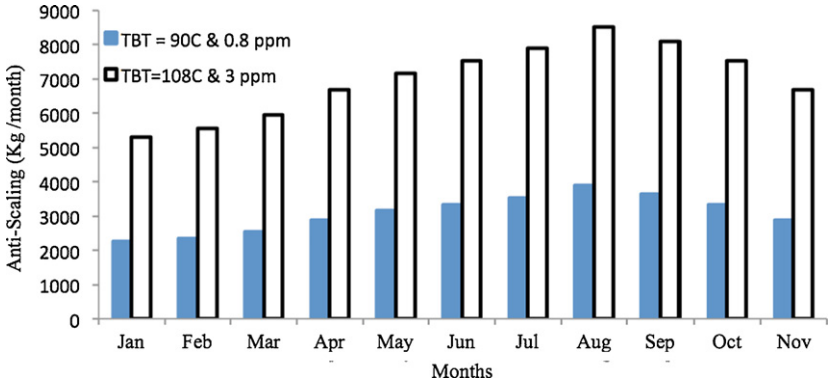

Fig. 14. Variation of optimal monthly anti-scaling consumption throughout the year.

$$C5 \quad (\text{Labour} \quad \text{cost}) = 8000 \times \left[\frac{D_N}{1000}\right] \times 0.1 \tag{29}$$

8.2. Case study

Here the effect of dynamic brine heater fouling on the performance of MSF process (in terms of GOR = D_N/W_{steam} and operating costs) is studied for a fixed demand fresh water $D_N = 9.45 \times 10^5$ kg/h. Two cases are considered. In Case 1, TBT = 90 °C with anti-scaling (polyphosphates) rate of 0.8 ppm is considered. In Case 2, TBT = 108 °C with anti-scaling rate of 3 ppm is considered. Note, the concentration (ppm) of H_2SO_4, Caustic soda and Chlorine are constant for both case studies.

The configuration investigated in this work refers to the case study reported by Rosso et al. [9]. The total number of stages is 16, with 13 stages in the recovery section and 3 in the rejection section. The specifications and constant parameters (except for f_{bh}), which are used in this work, are shown in Table 1. Seasonal variation of seawater temperature is shown in Tables 4 and 5 (based on [20]). For different seawater temperatures corresponding brine heater fouling factors are calculated using Eq. (23). The optimization problem OP is then solved for each $T_{seawater}$ and f_{bh} Tables 4 and 5 also show the optimal monthly operating cost, chemical required, steam consumption and the operating parameters such as make up, brine recycle flow rate, steam temperature and GOR throughout the year. Note, December is assumed to be overhauling period.

From January onward f_{bh} increases and so does the $T_{seawater}$. This consequently demands higher F and R and steam consumption (W_{steam}) leading to higher TOC (monthly) for both cases. However, with decrease in $T_{seawater}$ from August onward, F, R and TOC decrease (even though f_{bh} kept on increasing). Clearly, the effect of $T_{seawater}$ on F, R and TOC is more pronounced compared to the effect of f_{bh}. Note, the highest total TOC is noted in August at the maximum yearly $T_{seawater}$ (35 °C). For all cases, F and R vary significantly. Low TBT required higher R and F (compare the results in Table 4 with Table 5). Although there is a decrease (only slightly) in steam cost for Case 1, the total chemical cost is higher due to

higher requirement of F. The overall optimization results also show higher performance ratio GOR is achieved with higher TBT and chemical additives (see amount of anti-scale in Fig. 14). Although the operating cost is slightly lower in Case 2 (about 2.6%), the residual anti-scaling concentration present is higher in the brine blow down. It is expected that the impact on marine environment will be higher if this blow down is discharged to the sea without treatment.

Finally, note that at the same $T_{seawater}$ of 25 °C in April and November, although F and R remain the same, W_{steam}, T_{steam} and TOC increase due to increase in f_{bh}.

9. Conclusions

A simple linear dynamic brine heater fouling factor profile is developed based on actual MSF plant operation data. First, MSF model validation and sensitivity analysis of brine heater fouling and seawater temperature on the production of fresh water and other operating parameters such as top brine temperature, steam consumption, brine recycling and performance ratio are presented.

It can be seen from the results that increase of brine heater fouling by (90%) will cause a reduction in overall heat transfer coefficient and consequentially lowers TBT with fixed seawater temperature. This leads to a decrease in the fresh water production by (5.5%). The simulation also shows that for fixed freshwater demand and constant TBT, the higher the brine heater fouling factor, the higher steam consumption and the higher the steam temperature.

The simulation results also clearly show that it is possible to supply fixed fresh water demand throughout the year with changes in seawater temperature and brine heater fouling. Interesting observation shows that for a given brine heater fouling the top brine temperature decreases as seawater temperature increases. However, interestingly it can be noted that the plant can be operated successfully at lower top brine temperature (TBT) with higher steam consumption and higher brine recycling.

Even in summer time, the MSF process could fulfil the demand of fresh water by operating with lower top brine temperature, higher steam, higher brine recycle flow rate and lower performance. This will reduce scale formation rate and therefore the frequency of shutdown for cleaning will be lower and therefore the cost of maintenance will be lower. In this work, the performance ratio (GOR) does not reflect the maintenance cost.

Finally, the sensitivity of the fouling factor on the optimal performance of MSF process is studied at discrete time zone corresponding to different seawater temperature. Two different operations in terms of TBT and anti-scale dosing are considered. With freshwater demand fixed throughout the year, for each discrete time interval (season), the operating parameters such as make up flow rate, brine recycle flow rate and steam temperature are optimized while minimizing the total operation costs.

The optimization results clearly show that as the scale builds up with time, there will be increase in the steam temperature, steam consumption, brine flow rates, total operating costs and decrease in GOR even though the seawater temperature remains the same throughout the year. The variation in seawater temperature throughout the year together with changes in the brine heater fouling factor adds further changes in the operating parameters, costs and GOR. High TBT and anti-scaling dosing although preferable in terms of steam consumption and GOR, this will lead to further environmental impact.

References

[1] H.T. EL-Dessouky, H.M. Ettouney, Fundamentals of Salt Water Desalination, Elsevier Science Ltd., Amsterdam, 2002.
[2] M.K.A. AL-Sofi, Fouling phenomena in multi stage flash (MSF) distillers, Desalination 126 (1999) 61–76.
[3] J.S. Gill, A novel inhibitor for scale control in water desalination, Desalination 124 (1999) 43–50.
[4] N.H. Aly, A. El-Fiqi, Thermal performance of seawater desalination systems, Desalination 158 (2003) 127–142.
[5] W. EL-Moudir, M. ElBousiffi, S. Al-Hengari, Process modelling in desalination plant operations, Desalination 222 (2008) 431–440.
[6] S.F. Mussati, P.A. Aguirre, N.J. Scenna, A rigorous mixed-integer non lineal programming model (MINLP) for synthesis and optimal operation of cogeneration seawater desalination plants, Desalination 166 (2004) 339–345.
[7] M.S. Tanvir, I.M. Mujtaba, Optimization of design and operation of MSF desalination process using MINLP technique in gPROMS, Desalination 222 (2008) 419–430.
[8] A.E. Al-Rawajfeh, Simultaneous desorption-crystallization of CO_2–$CaCO_3$ in multi-stage flash (MSF) distillers, Chemical Engineering and Processing 47 (2008) 2269–2272.
[9] M. Rosso, A. Beltmmini, M. Mazzotti, M. Morbidelli, Modeling multistage flashdesalination plants, Desalination 108 (1996) 365–374.
[10] N.M. Wade, Distillation plant development and cost update, Desalination 136 (2001) 3–12.
[11] J.H. Beamer, D.J. Wilde, The simulation and optimization of a single effect multistage flashdesalination plant, Desalination 9 (1971) 259–275.
[12] K. Hayakawa, H. Satori, K. Konishi, Process simulation on multi flash desalination plant, in: 4th International Symposium on Fresh Water from Sea, vol. 1, 1973, p. 303.
[13] A.M. Helal, M.S. Medani, M. Soliman, J. Flower, A TDM model for MSF desalination plants, Comput. Chem. Eng. 10 (1986) 327–342.
[14] H.T. El-Dessouky, H.M. Ettouney, Simulation of combined multiple effect evaporation–vapor compression desalination processes, in: 1st IDA Int. Desalination Conference, Cairo, 1997.
[15] M.S. Tanvir, I.M. Mujtaba, Modelling and simulation of MSF desalination process using gPROMS and neural network based physical property correlation, Comput. Aided Chem. Eng. 21 (2006) 315–320.
[16] N.M. Abdel-Jabbar, H.M. Qiblawey, F.S. Mjalli, H. Ettouney, Simulation of large capacity MSF brine circulation plants, Desalination 204 (2007) 501–514.
[17] R.W. Stoughton, M.H. Lietzke, Thermodynamic properties of sea salt solutions, Chem. Eng. Data 12 (1967) 101–104.
[18] O.A. Hamed, M.A.K. AL-Sofi, G.M. Mustafa, A.G. Dalvi, Performance of different anti-scalants in multi-stage flash distillers, Desalination 123 (1999) 185–194.
[19] O.A. Hamed, M.A.K. AL-Sofi, M. Imam, K. Ba-Mardouf, A.S. AL-Mobayed, A. Ehsan, Evaluation of polyphosphonate anti-scalant at low dose rate in the ALJubail PhaseII MSF plant, Saudi Arabia, Desalination 128 (2000) 275–280.
[20] M. Abdel-Jawed, M. AL-Tabtabael, Impact of current power generation and water desalination activities on Kuwaiti marine environment, in: Proceedings of IDA World, 1999.
[21] A.M. Helal, A.M. El-Nashar, E. Al-Katheeri, S. Al-Malek, Optimal design of hybrid RO/MSF desalination plants. Part I. Modelling and algorithms, Desalination 154 (2003) 43–66.
[22] A.S. Nafey, H.E.S. Fath, A.A. Mabrouk, Thermo-economic investigation of multi effect evaporation (MEE) and hybrid multi effect evaporation—multi stage flash (MEE-MSF) systems, Desalination 201 (2006) 241–254.